AIMS Mathematics, 11(6): 15797–15816.
DOI: 10.3934/math.2026650
Received: 21 March 2026
Revised: 29 April 2026
Accepted: 21 May 2026
Published: 04 June 2026

https://www.aimspress.com/journal/Math

Research article

Dynamics of a delayed stage-structured fishery management model with impulsive nonlinear harvesting and impulsive birth

Shirui Zhang[1,2], **Jianjun Jiao**[1,2,*], **Guiyu Wu**[1,2] **and Bingying Gao**[1,2]

[1] School of Mathematics and Statistics, Guizhou University of Finance and Economics, Guiyang 550025, China

[2] School of Big Data Statistics, Guizhou University of Finance and Economics, Guiyang 550025,China

* **Correspondence:** Email: jiaojianjun2018@126.com; Tel: +8618985017112.

Abstract: Irrational fishing strategies have endangered numerous fish species. The density-dependent harvesting strategy has emerged as one of the potent approaches to address this issue. In this paper, we formulate a fishery management model incorporating the Beddington-DeAngelis functional response and delayed stage structure. The prey population is seasonal birth and impulsive nonlinear harvesting at distinct times. Initially, we show the positivity and the uniform boundedness of solutions in the system. By the comparison theorem of impulsive differential equations, we obtain the global attractivity conditions for the predator-extinction periodic solution. Sufficient conditions for the persistence of the system are derived via constructing the Lyapunov functions and applying other analytical methods. The numerical simulations demonstrate our findings and indicate that impulsive effects, impulsive period and maturation delay have significant influences on the dynamical behaviors of the system. These results provide certain theoretical guidance for sustainable fisheries.

Keywords: fishery management; impulsive nonlinear harvesting; delayed stage-structure; Beddington-DeAngelis functional response; impulsive birth
Mathematics Subject Classification: 34D23, 37M05, 92D25

1. Introduction

Abundant biological resources constitute the material basis for the development of human society and fall into three major categories: animal (especially fishery resources), plant and microbial resources. During industrial civilization, ecological balance has been severely damaged due to one-sided pursuit of economic growth and unrestrained exploitation of biological resources. This has led to widespread environmental pollution, loss of biodiversity and more frequent extreme weather events.

Given these situations, the sustainable development has become global consensus and prompts us to focus on more efficient and eco-friendly resource control strategies.

The ocean, covering approximately seventy percent of the earth's surface, serves as an important source of diverse minerals and marine products. In recent decades, due to overfishing and environmental pollution, many fish populations have declined drastically and are at even greater risk of extinction. For example, the Yangtze finless porpoise, the red stingray from the Xijiang River Basin in Guangxi and the bluefin tuna are listed as endangered species. To predict the population variations under external environmental changes and human disturbances, mathematical models have received extensive attention in population ecology. Among these, ordinary differential equations (ODE) are frequently employed to describe continuous-time population dynamics and reveal the inherent laws of interspecific interactions and have been applied in other research fields [1, 2]. To date, many scholars have conducted extensive modeling research on the dynamic properties of fishery populations subject to fishing and environmental perturbations [3–5], among which the harvest is one of the indispensable factors to be considered. Zhang [6] established a reaction–diffusion–advection model with a variable habitat for predator and fully characterized the global dynamical behavior of the system for Holling type I and II functional responses. Bo, Lv and Liu [7] constructed a fishery predator-prey system considering stage structure and additional food and given the threshold of additional food required to maintain the permanence as well as the optimal harvesting strategy. Zhou [8] focused on an aquaculture model with impulsive harvesting and nonlinear density-dependent stocking and portrayed the dynamic transition from predator extinction to prey-predator coexistence using the stroboscopic map, Floquet's theory and bifurcation analysis. Constrained by resource conditions and population size, continuous harvesting is overly idealistic in practical production. Furthermore, the impact of fishing activities on fish populations is usually instantaneous. Therefore, in this paper, we will employ impulsive differential equations to describe fishing behavior, which is more reasonable and reliable.

With the development of mathematical models for ecology, an increasing array of factors need to be incorporated to improve realism, such as interspecific interactions, stage structure and seasonal birth pulses. Most organisms exhibit distinct physiological traits across life cycle stages and are thus commonly divided into immature and mature stages [9–11]. For instance, juveniles depend on parental care and neither hunt nor reproduce. It takes certain time for juveniles to grow into adults (i.e. maturation delay) and juveniles may die due to various causes during this period. In stage-structured models without maturation delays, it is often assumed that immature individuals develop into adults at a constant rate, while the developmental duration required for this process and the potential mortality are neglected. For stage-structured models without time delay, it is commonly assumed that immature individuals develop into adults at a fixed rate, with the requisite developmental duration and potential mortality rates overlooked in the process. In nature, no organism can survive in isolation. A variety of complex interspecific interactions, including competition, mutualism, predation and parasitism, are commonly observed. In particular, the predator–prey relationship remains a central research focus in ecological studies [12, 13]. The functional responses serve as the bridge to better understand the complex predator-prey relationship, which express that each predator can harvest the number of prey per unit time. Arditi [14] and Huisman [15] mentioned "prey-dependent" type functional responses, who argued that the predation rate is mainly related to the prey density.However, predatory activities are affected not only by prey density but also by predator density in reality. In 1975, Beddington [16] and DeAngelis [17] independently proposed the Beddington-DeAngelis (B-D) functional response

resembling the Holling-II type [18], which incorporates an additional term that renders it more consistent with real-world scenarios [19–21]. In addition, taking the seasonal birth into account is necessary in the model of this paper. For the mandarin fish, it typically engages in mass spawning when water temperatures rise moderately. Given that its breeding period is considerably shorter than its overall life cycle, we can regard the reproductive behavior as a pulsed process. Quan [22] systematically considered transient and nontransient pulse births and incorporated pulsed stocking and harvesting of prey to establish a system with multiple pulse effects, finding that a larger pulse birth intensity is more conducive to prey proliferation and predator persistence.

In light of the aforementioned factors, we are going to build a delayed stage-structured fishery management model incorporating the B-D functional response, impulsive birth and nonlinear harvesting at various moments. The particular model will be set forth in Section 2. Then, we will introduce and attest the crucial lemmas and theorems needed for the subsequent analysis in Section 3. For section 4, the sufficient conditions leading to the global attractivity of the periodic solution in which the predator population goes extinct and the system's persistence are presented. In Section 5, numerical simulations serve to validate the outcomes and explore the influence of several vital parameters on the system. In closing, Section 6 provides a brief conclusion.

2. Model formulation

Researchers employ mathematical parameters to characterize population traits (growth, death, competition) and establish population dynamics models to describe how population density changes over time. Harvesting behavior is a major focus in fishery-related modeling and is usually abstracted as either continuous or impulsive harvesting for analysis. Ling and Wang [23] studied the predator-prey model with continuous harvesting:

$$\begin{cases} \dot{x}_i = x_i f(x_i) - y_i g(x_i, y_i) - h, \\ \dot{y}_i = h\,[g(x_i, y_i), v]\, y_i, \end{cases} \tag{2.1}$$

where x_i and y_i denote the quantity of prey and natural enemy population, respectively. $f(x_i) = 1 - x_i$ is expressed as the natality of prey population and $g(x_i, y_i) = 1 - e^{-rx_i}$ corresponds to the Ivlev-type functional response. The per-capita growth rate for predator is defined as $h[g(x_i, y_i), y_i] = \varepsilon g(x_i, y_i) - \beta$. Here, β signifies the individual death rate of predator as well as ε stands for the transformation efficiency from food into offspring. Moreover, h is non-negative and indicates the rate of harvesting or removal.

However, numerous factors, such as the limited reproductive capacity and resources required for fishing, make the continuous harvesting infeasible in practical operation. Therefore, some scholars have employed impulse differential equations to analyze the dynamic properties of populations with

harvesting behavior. Notably, Jiao [24] proposed the model given below:

$$\begin{cases} \left.\begin{aligned} \frac{\mathrm{d}x_j(t)}{\mathrm{d}t} &= x_j(t)(a - bx_j(t)) - \beta x_j(t)y_j(t), \\ \frac{\mathrm{d}y_j(t)}{\mathrm{d}t} &= k\beta x_j(t)y_j(t) - dy_j(t), \end{aligned}\right\} \ t \neq (n+k)\hat{T},\ t \neq (n+1)\hat{T}, \\ \left.\begin{aligned} x_j(t^+) &= (1-\mu_1)x_j(t), \\ y_j(t^+) &= (1-\mu_2)y_j(t), \end{aligned}\right\} \ t = (n+k)\hat{T},\ n = 1, 2, \ldots, \\ \left.\begin{aligned} x_j(t^+) &= x_j(t) + \mu, \\ y_j(t^+) &= y_j(t), \end{aligned}\right\} \ t = (n+1)\hat{T},\ n = 1, 2, \ldots, \end{cases} \tag{2.2}$$

where $x_j(t)$ and $y_j(t)$ denote the population sizes of the prey and predator at time t. μ_1 and $\mu_2 \in (0, 1)$ stand for the harvesting rate of the prey X_j and the predator Y_j at $t = (n+k)\hat{T}$, respectively. $\mu > 0$ indicates the number of the prey X_j released at $t = (n+1)\hat{T}$. For the specific definitions of other parameters, one can refer to [24].

Wu [25] hypothesized that the life cycle of prey population (pest) can be divided into two stages based on physiological features and established a pest control model integrating delayed stage structure and impulsive nonlinear release for natural enemies, which provides assistance for the biological control of pests:

$$\begin{cases} \left.\begin{aligned} \frac{dx_{11}^*(t)}{dt} &= ax_{21}^*(t) - \theta x_{11}^*(t) - ae^{-\theta\tau}x_{21}^*(t-\tau), \\ \frac{dx_{21}^*(t)}{dt} &= ae^{-\theta\tau}x_{21}^*(t-\tau) - dx_{21}^*(t) - \frac{\beta x_{21}^*(t)y^*(t)}{1+\mu x_{21}^*(t)} - d_1(x_{21}^*(t))^2, \\ \frac{dy_1^*(t)}{dt} &= \frac{k\beta x_{21}^*(t)y_1^*(t)}{1+\mu x_{21}^*(t)} - cy_1^*(t), \end{aligned}\right\} \ t \neq n\hat{T}, \\ \left.\begin{aligned} x_{11}^*(t^+) &= x_{11}^*(t), \\ x_{21}^*(t^+) &= x_{21}^*(t), \\ y_1^*(t^+) &= y_1^*(t) + \frac{h_{\max}}{1+\xi y_1^*(t)}, \end{aligned}\right\} \ t = n\hat{T}, \end{cases} \tag{2.3}$$

where $x_{11}^*(t)$, $x_{21}^*(t)$ and $y_1^*(t)$ signify the population quantities of the juvenile pest, adult pest and natural enemy in the rice crop field, respectively. Here, θ stands for the mortality rate, and a represents the natality of the immature pest. The term $ae^{-\theta\tau}x_2(t-\tau)$ denotes the individuals maturing from immaturity to adulthood. Further details can be found in [25].

In this paper, we consider impulsive nonlinear harvesting similar to the nonlinear control strategy for integrated pest management proposed by Li [26],

$$f(t, x_r) = -\frac{\delta x_r(t)}{x_r(t) + h}.$$

When the pest population $x_r(t)$ is extremely small, almost no pesticide is required. As the pest population increases, the spraying intensity rises correspondingly, eventually becoming saturated and stopping further increase. Here, $h \geq 0$ and $1 > \delta > 0$ denote the half-saturation coefficient and the

maximal fatality rate on the pest.

Drawing on the above discussion, we assume that the prey population is seasonally born and is subjected to periodic nonlinear harvesting, and accordingly split the life cycle of the predator population into two major stages for exploration. That is to say, the delayed stage structure, impulsive birth, and pulse nonlinear harvesting are introduced into the predator-prey system featuring the Beddington-DeAngelis functional response:

$$\begin{cases} \left.\begin{aligned} \frac{dx(t)}{dt} &= -\mu x(t) - \frac{\beta x(t) y_2(t)}{1+\alpha x(t)+c y_2(t)}, \\ \frac{dy_1(t)}{dt} &= \frac{k\beta x(t) y_2(t)}{1+\alpha x(t)+c y_2(t)} - d y_1(t) - k\beta e^{-d\tau} \frac{x(t-\tau) y_2(t-\tau)}{1+\alpha x(t-\tau)+c y_2(t-\tau)}, \\ \frac{dy_2(t)}{dt} &= k\beta e^{-d\tau} \frac{x(t-\tau) y_2(t-\tau)}{1+\alpha x(t-\tau)+c y_2(t-\tau)} - d_1 y_2(t) - d_2 y_2^2(t), \end{aligned} \right\} \ t \neq (n+l-1)T,\ t \neq nT, \\ \left.\begin{aligned} x(t^+) &= (1+p)x(t), \\ y_1(t^+) &= y_1(t), \\ y_2(t^+) &= y_2(t), \end{aligned} \right\} \ t = (n+l-1)T, \\ \left.\begin{aligned} x(t^+) &= \left(1 - \frac{\lambda_{max} x(t)}{\delta + x(t)}\right) x(t), \\ y_1(t^+) &= y_1(t), \\ y_2(t^+) &= y_2(t), \end{aligned} \right\} \ t = nT. \end{cases} \tag{2.4}$$

The initial condition of system (2.4) is as follows:

$$(\psi_1^*(\varkappa), \psi_2^*(\varkappa), \psi_3^*(\varkappa)) \in C_+ = C\left([-\tau, 0], R_+^3\right) \quad \psi_k(0) > 0, k = 1, 2, 3. \tag{2.5}$$

Here, $x(t)$, $y_1(t)$ and $y_2(t)$ denote the population quantities of prey, juvenile and adult predator, respectively. The juvenile predators require a fixed time τ to mature into adults. During the immature stage, individuals neither hunt nor reproduce, and experience no competitive interactions and may die from natural or external factors. In addition, the prey population reproduces at a birth rate p at $t = (n+l-1)T$ and is harvested at moment $t = nT$ $(0 < l < 1, n \in Z^+)$. It is evident that $\frac{\lambda_{\max} x(t)}{\delta + x(t)} \to 0$ as $x(t) \to 0$ and $\frac{\lambda_{\max} x(t)}{\delta + x(t)} \to \lambda_{\max}$ as $x(t) \to \infty$. In other words, the harvesting intensity is dependent on the density of the prey population. The detailed parameter descriptions of the system (2.4) are shown in Table 1.

Table 1. Biological interpretations of parameters in system (2.4).

Parameter	Biological implication	Dimension
μ	Mortality rate of prey	time^{-1}
β	The predation rate	time^{-1}
α	Half-saturation constant	biomass^{-1}
c	Half-saturation constant	biomass^{-1}
k	Conversion efficiency of prey to juvenile predator	biomass
d	Mortality rate of juvenile predator	time^{-1}
d_1	Mortality rate of adult predator	time^{-1}
τ	Maturation delay	time
d_2	Intraspecific competition rate of adult predator	biomass^{-1}time^{-1}
T	Impulsive period	time
p	Birth rate of prey	–
$\lambda_{\max}$	Maximum harvesting effort	–
δ	Half-saturation constant	biomass

We simplify system (2.4) to gain the following system:

$$\begin{cases} \left.\begin{aligned} &\frac{dx(t)}{dt} = -\mu x(t) - \frac{\beta x(t) y_2(t)}{1 + \alpha x(t) + c y_2(t)}, \\ &\frac{dy_2(t)}{dt} = k\beta e^{-d\tau} \frac{x(t-\tau) y_2(t-\tau)}{1 + \alpha x(t-\tau) + c y_2(t-\tau)} - d_1 y_2(t) - d_2 y_2^2(t), \end{aligned}\right\} \ t \neq (n+l-1)T, \ t \neq nT, \\ \left.\begin{aligned} &x(t^+) = (1+p)x(t), \\ &y_2(t^+) = y_2(t), \end{aligned}\right\} \ t = (n+l-1)T, \\ \left.\begin{aligned} &x(t^+) = \left(1 - \frac{\lambda_{max} x(t)}{\delta + x(t)}\right) x(t), \\ &y_2(t^+) = y_2(t), \end{aligned}\right\} \ t = nT, \\ (\psi_1^*(\varkappa), \psi_3^*(\varkappa)) \in C_+ = C([-\tau, 0], R_+^2) \quad \psi_i(0) > 0, i = 1, 3. \end{cases} \tag{2.6}$$

3. Preliminaries

Suppose $F(t) = (x(t), y_1(t), y_2(t))^T$ is the solution to system (2.4). Let $F : R_+ \times R_+^3 \to R_+$ be piecewise continuous and of class C^1 on $((n-1)T, (n+l-1)T] \times R_+^3$ and $((n+l-1)T, nT] \times R_+^3$ for all $n \in N$, and $\lim_{(t,x)\to((n+l-1)T^+,X)} F(t,x) = F((n+l-1)T^+, X)$, $\lim_{(t,x)\to(nT^+,X)} F(t,x) = F(nT^+, X)$ exist. The smoothness properties of f_1^*, which represents the mapping corresponding to the right part of the first three equations of system (2.4), guarantee the global existence and uniqueness of the solution for system (2.4).

Definition 3.1. Model (2.6) is deemed permanent if there exists a compact region $D \subset \text{int}R_+^2$ with the property that all solutions $(x(t), y_2(t))$ of model (2.6) ultimately enter and stay within region D for enough large t.

Lemma 3.2. *Suppose the following inequalities hold [27]:*

$$\begin{cases} D^+F(t,x) \le f(t,F(t,x)), \ \ t \ne (n+l-1)T, \ t \ne nT, \\ F(t,x(t^+)) \le \psi(F(t,x)), \ \ t = (n+l-1)T, \\ F(t,x(t^+)) \le \phi(F(t,x)), \ \ t = nT. \end{cases} \tag{3.1}$$

Here, the function $f : R_+ \times R_+ \to R$ is continuous on the intervals $((n-1)T,(n+l-1)T]$ and $((n+l-1)T,nT]$. For any $n \in N$, $\lim_{(t,x)\to((n+l-1)T^+,y)} f(t,x) = f((n+l-1)T^+,y)$, $\lim_{(t,x)\to(nT^+,y)} f(t,x) = f(nT^+,y)$ exist. Additionally, $\psi,\phi : \mathbb{R}_+ \to \mathbb{R}_+$ are non-decreasing functions. Let $h(t)$, defined on $[0,\infty)$, be the maximal solution of the scalar impulsive differential equation

$$\begin{cases} \dot{H}(t) = f(t,H(t)), \ \ t \ne (n+l-1)T, \ t \ne nT, \\ H(t^+) = \psi(H(t)), \ \ t = (n+l-1)T, \\ H(t^+) = \phi(H(t)), \ \ t = nT, \\ H(0^+) = H_0. \end{cases} \tag{3.2}$$

Then, if $F(0^+,x_0) \le H_0$, it follows that $F(t,x) \le h(t)$ for all $t \ge 0$.

Lemma 3.3. *Suppose p, q, and τ are positive constant. $x^*(t) > 0$ is the subsequent delayed differential equation' solution:*

$$\frac{dx^*(t)}{dt} = px^*(t-\tau) - qx^*(t), \ \phi^*(\varkappa) \in C([-\tau,0],R_+), \ \phi^*(0) > 0.$$

(i) When $p < q$, $\lim_{t\to\infty} x^*(t) = 0$.
(ii) When $p > q$, $\lim_{t\to\infty} x^*(t) = +\infty$.

Theorem 3.4. *For $t > 0$, the solutions of system* (2.4) *under the starting condition* (2.5) *take on positive values.*

Proof. First, we demonstrate that $x(t) > 0$ holds for $t \in (0,T]$. Owing to the solution's existence and uniqueness, by the first equation of system (2.4), we can infer

$$x(t) = x(0^+)\exp\left(-\int_0^t \mu + \frac{\beta y_2(\zeta)}{1+\alpha x(\zeta)+cy_2(\zeta)}d\zeta\right) > 0, \ \ t \ne lT, \ t \ne T. \tag{3.3}$$

Thus,

$$x(lT^+) = (1+p)x(lT) > 0,$$

and

$$x(T^+) = \left(1 - \frac{\lambda_{max}x(T)}{\delta + x(T)}\right)x(T) = \left(1 - \frac{\lambda_{max}\exp(\vartheta)x(0^+)}{\delta + \exp(\vartheta)x(0^+)}\right)\exp(\vartheta)x(0^+) > 0,$$

where $\vartheta = -\int_0^T \mu + \frac{\beta y_2(s)}{1+\alpha x(s)+cy_2(s)}ds$. Hence, $x(t)$ is positive for $t \in (0,T]$. Then, due to $x(T^+) > 0$, we further derive that $x(t) > 0$ within the interval $t \in (T,2T]$. By analogy, the $x(t)$ is positive for $t > 0$.

Now, our goal is to verify that $y_2(t) > 0$ when $t > 0$. Assume there is a t_0 that satisfies $y_2(t_0) = 0$ and $t_0 = \inf\{t > 0 : y_2(t) = 0\}$. Moreover, by plugging t_0 into the third equation of system (2.4), we obtain

$$\dot{y}_2(t_0) = k\beta e^{-d\tau}\frac{x(t_0-\tau)y_2(t_0-\tau)}{1+\alpha x(t_0-\tau)+cy_2(t_0-\tau)} > 0. \tag{3.4}$$

There exists a enough small $\varepsilon > 0$, making $\dot{y}_2(t_0 - \varepsilon) > 0$ valid as well. Nevertheless, according to the specification of t_0, $\dot{y}_2(t_0 - \varepsilon) \leq 0$ holds, which leads to a contradiction. Thus, $y_2(t) > 0$ is true for $t > 0$.

Before testifying that $y_1(t) > 0$ for $t > 0$, it needs to be pointed out

$$y_1(k\tau) = \int_{(k-1)\tau}^{k\tau} k\beta e^{d(\varsigma - k\tau)} \frac{x(\varsigma)y_2(\varsigma)}{1 + \alpha x(\varsigma) + cy_2(\varsigma)} d\varsigma, \quad k = 0, 1, 2, \ldots. \tag{3.5}$$

We next present the subsequent equation:

$$\dot{U}(t) = -dU(t) - k\beta e^{-d\tau} \frac{x(t-\tau)y_2(t-\tau)}{1 + \alpha x(t-\tau) + cy_2(t-\tau)}, \quad U(k\tau) = y_1(k\tau). \tag{3.6}$$

Through a simple calculation, we acquire

$$U(t) = e^{-d(t-k\tau)} \left[U(k\tau) - \int_{k\tau}^{t} k\beta e^{d(\zeta - (k+1)\tau)} \frac{x(\zeta - \tau)y_2(\zeta - \tau)}{1 + \alpha x(\zeta - \tau) + cy_2(\zeta - \tau)} d\zeta \right]. \tag{3.7}$$

It can be readily shown that $U((k+1)\tau) = 0$. We observe that if $U(t)$ denotes the solution of Eq (3.6) and $y_1(t)$ satisfies the second equation within system (2.4), then $y_1(t) > U(t)$. Given that $U(t)$ is strictly decreasing, we further conclude that $y_1(t) > 0$ for $t \in [k\tau, (k+1)\tau]$. Thereby, the positivity is demonstrated.

Consider the following model:

$$\begin{cases} \dot{g}(t) = -\mu g(t), \quad t \neq (n + l - 1)\hat{T}, \ t \neq n\hat{T}, \\ g(t^+) = (1 + p)g(t), \quad t = (n + l - 1)\hat{T}, \\ g(t^+) = \left(1 - \dfrac{\lambda_{max} g(t)}{\delta + g(t)}\right) g(t), \quad t = n\hat{T}. \end{cases} \tag{3.8}$$

To begin with, the specific expression of solution of model (3.6) for $t \in \left((n-1)\hat{T}, n\hat{T}\right]$ is as follows:

$$g(t) = \begin{cases} g((n-1)\hat{T}^+)e^{-\mu(t-(n-1)\hat{T})}, & t \in ((n-1)\hat{T}, (n+l-1)\hat{T}], \\ g((n+l-1)\hat{T}^+)e^{-\mu(t-(n+l-1)\hat{T})}, & t \in ((n+l-1)\hat{T}, n\hat{T}], \end{cases} \tag{3.9}$$

which results in the stroboscopic map

$$g(n\hat{T}^+) = (1 + p)e^{-\mu\hat{T}} g((n-1)\hat{T}^+) \left(1 - \frac{\lambda_{max}(1 + p)e^{-\mu\hat{T}} g((n-1)\hat{T}^+)}{\delta + (1 + p)e^{-\mu\hat{T}} g((n-1)\hat{T}^+)}\right). \tag{3.10}$$

Let $g_n = g(n\hat{T}^+)$ and $\hat{\omega} = (1 + p)e^{-\mu\hat{T}} > 0$, we can obtain

$$g_n = \hat{\omega} g_{n-1} \left(1 - \frac{\lambda_{max}\hat{\omega} g_{n-1}}{\delta + \hat{\omega} g_{n-1}}\right) \triangleq F(g_{n-1}). \tag{3.11}$$

When $\hat{\omega} < 1$, then the equation (3.11) has a trivial equilibrium point $g_1^* = 0$, which is local stability since

$$\left|\frac{dF(g)}{dg}\right|_{g=g_1^*} = (1 + p)\exp(-\mu\hat{T}) = \hat{\omega} < 1.$$

Moreover, Eq (3.11) has another positive fixed point $g_2^* = \frac{\delta(1-\hat{\omega})}{(1-\lambda_{max})\hat{\omega}^2-\hat{\omega}}$, which is locally stable attributed to

$$\left|\frac{dF(g)}{dg}\right|_{g=g_2^*} = \left|\frac{\hat{\omega}^2(1-\lambda_{max}) - 2\hat{\omega}(1-\lambda_{max}) + 1}{\hat{\omega}\lambda_{max}}\right| < 1,$$

where $\hat{\omega} > 1$ and $\lambda_{max} > 1 - \frac{1}{\hat{\omega}}$.

During the following discussion, we will demonstrate the equilibrium point g^* of Eq (3.11) is global asymptotic stability, provided that the below-stated conditions are met:

(a) if $g^* > g > 0$, we have $g^* > F(g) > g$;

(b) if $g > g^*$, we have $g > F(g) > g^*$.

With regard to

$$\dot{F}(g) = \frac{(1-\lambda)\hat{\omega}^3 g^2 + 2(1-\lambda)\delta\hat{\omega}^2 g + \delta^2\hat{\omega}}{(\delta+\hat{\omega}g)^2} > 0, \tag{3.12}$$

it is clear that $g^* > F(g)$ as $g^* > g > 0$. Subsequently, we can derive that $\dot{G}(g) = -\frac{\lambda_{max}\delta\hat{\omega}^2}{(\delta+\hat{\omega}x)^2} < 0$ by defining $G(g) = F(g)/g$. It is not difficult to find $F(g) > g$ under the condition that $g^* > g > 0$. Similarly, when $g > g^*$, we can conclude that $g > F(g) > g^*$. Thus, the statements (a) and (b) are fulfilled, and then fixed points g_1^* and g_2^* of Eq (3.11) are globally asymptotically stable.

Theorem 3.5. *Let $\hat{\omega} = (1+p)\exp(-\mu\hat{T})$. When $\hat{\omega} < 1$, model* (3.8) *admits the trivial periodic solution $\widetilde{g_1}(t) = 0$, which is globally asymptotically stable. On the other hand, if $\hat{\omega} > 1$ and $\lambda_{max} > 1 - \frac{1}{\hat{\omega}}$, model* (3.8) *possesses another positive periodic solution $\widetilde{g_2}(t)$. This solution is also globally asymptotically stable, and its explicit expression is presented as follows:*

$$\widetilde{g_2}(t) = \begin{cases} \left(\dfrac{\delta(1-\hat{\omega})}{(1-\lambda_{max})\hat{\omega}^2-\hat{\omega}}\right)e^{-\mu(t-(n-1)\hat{T})}, & t \in ((n-1)\hat{T}, (n+l-1)\hat{T}], \\ (1+p)\left(\dfrac{\delta(1-\hat{\omega})}{(1-\lambda_{max})\hat{\omega}^2-\hat{\omega}}\right)e^{-\mu(t-(n-1)\hat{T})}, & t \in ((n+l-1)\hat{T}, n\hat{T}]. \end{cases} \tag{3.13}$$

Theorem 3.6. *The solution in system* (2.4) *is uniformly bounded.*

Proof. Defining $V_r(t) = kx(t) + y_1(t) + y_2(t)$ for $t \neq (n+l-1)T$ and $t \neq nT$, we gain

$$\begin{aligned} D^+V_r(t) + qV_r(t) &= -k(\mu-q)x(t) - (d-q)y_1(t) - (d_1-q)y_2(t) - d_2y_2^2(t) \\ &\leq -(d_1-q)y_2(t) - d_2y_2^2(t) \\ &\leq Q, \end{aligned}$$

where $q = \min\{\mu, d\}$ and $Q = (d_1-q)^2/4d_2$.

When $t = (n+l-1)T$, by taking the first equation of system (2.4) into account, we can obtain $\dot{x}(t) \leq -\mu x(t)$. Next, we establish the subsequent model:

$$\begin{cases} \dot{h}_1(t) = -\mu h_1(t), & t \neq (n+l-1)T, nT, \\ h_1(t^+) = (1+p)h_1(t), & t = (n+l-1)T, \\ h_1(t^+) = \left(1 - \dfrac{\lambda_{max}h_1(t)}{\delta+h_1(t)}\right)h_1(t), & t = nT. \end{cases} \tag{3.14}$$

By Theorem 3.5, model (3.14) admits a positive periodic solution with global asymptotic stability,

$$\widetilde{h_1}(t) = \begin{cases} \left(\dfrac{\delta(1-\omega)}{(1-\lambda_{max})\omega^2-\omega}\right)e^{-\mu(t-(n-1)T)}, & t \in ((n-1)T,(n+l-1)T], \\ (1+p)\left(\dfrac{\delta(1-\omega)}{(1-\lambda_{max})\omega^2-\omega}\right)e^{-\mu(t-(n-1)T)}, & t \in ((n+l-1)T,nT], \end{cases} \tag{3.15}$$

where $\omega = (1+p)\exp(-\mu T)$. From the comparison theorem, there exists a enough small $\varepsilon_1 > 0$ and an integer T_1, which let $x(t) \le h_1(t) \le \widetilde{h_1}(t) + \varepsilon_1,\ t > T_1$. In particular, $x((n+l-1)T) \le a = \frac{\delta(1-\omega)}{(1-\lambda_{max})\omega^2-\omega}$, we obtain

$$\begin{aligned} V_r((n+l-1)T^+) &= V_r((n+l-1)T) + kpx((n+l-1)T) \\ &\le V_r((n+l-1)T) + kpa. \end{aligned}$$

For $t = nT$, $V_r(t)$ satisfies:

$$V_r(nT^+) = V_r - k\frac{\lambda_{\max}}{1+\delta x(nT)} \le V_r(nT).$$

Combining these, we derive that:

$$\begin{aligned} V_r(t) &\le V_r(0^+)e^{-qt} + \frac{Q}{q}(1-\exp(-qt)) + kpa\frac{\exp(-q(t-T)) - e^{-q(t-nT)}}{1-e^{qt}} \\ &\to \frac{Q}{q} + \frac{kpa}{\exp(qT)-1}, \quad t \in ((n-1)T,nT],\ n \to \infty. \end{aligned}$$

It follows that $V_r(t)$ is uniformly bounded. In light of the delineation of $V_r(t)$, there has to be a positive number M such that $x(t) \le M/k$, $y_1(t) \le M$, and $y_2(t) \le M$ as t is sufficiently large. Thus, the boundedness has been proved.

4. Major results

4.1. Global attraction predator-extinction periodic solution

Theorem 4.1. *Assume $L_1 = \frac{d_1}{k\beta\eta_1^* e^{-d\tau}} > 1$, in which $\eta_1^* = (1+p)\left(\frac{\delta(1-\omega)}{(1-\lambda_{max})\omega^2-\omega}\right)e^{-\mu lT}$. Under this condition, the predator-extinction periodic solution $(\widetilde{x_2}(t), 0)$ possesses globally attraction.*

Proof. For $L_1 > 1$, we can have $d_1 > k\beta(\eta_1^* + \varepsilon_1)e^{-d\tau}$. From Theorem 3.5 and the prior proof, We can infer that

$$x(t) \le \widetilde{h_1}(t) + \varepsilon_1 = \widetilde{x_2}(t) + \varepsilon_1,\ t \in ((n-1)T,nT],\ n > T_1.$$

Thus,

$$x(t) \le \begin{cases} \dfrac{\delta(1-\omega)}{(1-\lambda_{max})\omega^2-\omega} + \varepsilon_1, & t \in ((n-1)T,(n+l-1)T], \\ (1+p)\left(\dfrac{\delta(1-\omega)}{(1-\lambda_{max})\omega^2-\omega}\right)e^{-\mu lT} + \varepsilon_1, & t \in ((n+l-1)T,nT], \end{cases} \tag{4.1}$$

then we have $x(t) \le \eta_1 = (1+p)\left(\frac{\delta(1-\omega)}{(1-\lambda_{max})\omega^2-\omega}\right)e^{-\mu lT} + \varepsilon_1,\ t \in ((n-1)T, nT],\ \ n > T_1$.

Considering the second equation in the model (2.6), we gain that $\dot{y}_2(t) \le k\beta e^{-d\tau}\eta_1 y_2(t-\tau) - d_1 y_2(t)$, while defining the relevant comparison equation

$$h_2(t) = k\beta e^{-d\tau}\eta_1 h_2(t-\tau) - d_1 h_2(t),\ t > (n-1)T + \tau,\ n > T_1. \tag{4.2}$$

Since $d_1 > k\beta\eta_1 e^{-d\tau}$, we have $\lim_{t\to\infty} h_2(t) = 0$ according to Lemma 3.3. Hence, there exist a enough small $\varepsilon_2 > 0$ and a positive integer $T_2 > T_1$, so that $y_2(t) \le \varepsilon_2$ holds for all $t > T_2$.

Taking it into the first equation in model (2.6), we can derive $\dot{x}(t) \ge -(\mu + \beta\varepsilon_2)x(t)$ when $t > T_2$. Then, there must be $x(t) \ge \widetilde{h_3}(t)$ for $t \in ((n-1)T, nT]$ with $n > T_2$, where $\widetilde{h_3}(t)$ is only positive periodic solution of

$$\begin{cases} \dot{h}_3(t) = -(\mu+\beta\varepsilon_2)h_3(t), & t \ne (n+l-1)T,\ nT, \\ h_3(t^+) = (1+p)h_3(t), & t = (n+l-1)T, \\ h_3(t^+) = \left(1 - \dfrac{\lambda_{max}h_3(t)}{\delta + h_3(t)}\right)h_3(t), & t = nT. \end{cases} \tag{4.3}$$

Explicitly,

$$\widetilde{h_3}(t) = \begin{cases} \left(\dfrac{\delta(1-\omega_1)}{(1-\lambda_{max})\omega_1^2 - \omega_1}\right)e^{-\mu_1(t-(n-1)T)}, & t \in ((n-1)T, (n+l-1)T], \\ (1+p)\left(\dfrac{\delta(1-\omega_1)}{(1-\lambda_{max})\omega_1^2 - \omega_1}\right)e^{-\mu_1(t-(n-1)T)}, & t \in ((n+l-1)T, nT], \end{cases} \tag{4.4}$$

where $\mu_1 = \mu + \beta\varepsilon_2$ and $\omega_1 = (1+p)e^{\mu_1 T}$. For $t > T_3 > T_2$, $x(t) \ge \widetilde{h_3}(t) - \varepsilon_3$. Letting $\varepsilon_2 \to 0$, then we can infer $x(t) \ge \widetilde{x_2}(t) - \varepsilon_3$.

Based on the foregoing discussions, it can be deduce that $(x(t), y_2(t))$ converges to $(\widetilde{x_2}(t), 0)$ as t approaches infinity. The predator-extinction periodic solution of model (2.6) exhibits global attractivity. Thus, the justification comes to an end.

4.2. The uniform permanence

Theorem 4.2. *Assume* $L_2 = \frac{d_1}{k\beta\eta_2^* e^{-d\tau}}(1 + \alpha(M/k) + cM) < 1$, *in which* $\eta_2^* = \left(\frac{\delta(1-\omega_2)}{(1-\lambda_{max})\omega_2^2-\omega_2}\right)e^{-\mu_2 lT}$. *Under this condition, then model* (2.6) *is permanent.*

Proof. Rewrite the second equation in the model (2.6) as:

$$\dot{y}_2(t) = k\beta e^{-d\tau}\frac{x(t)y_2(t)}{1+\alpha x(t)+cy_2(t)} - d_1 y_2(t) - d_2 y_2^2(t) - k\beta e^{-d\tau}\frac{d}{dt}\int_{t-\tau}^{t}\frac{x(s)y_2(\zeta)}{1+\alpha x(\zeta)+cy_2(\zeta)}d\zeta.$$

Defining

$$W(t) = y_2(t) + k\beta e^{-d\tau}\int_{t-\tau}^{t}\frac{x(\zeta)y_2(\zeta)}{1+\alpha x(\zeta)+cy_2(\zeta)}d\zeta, \tag{4.5}$$

and computing the derivative of $W(t)$, we can gain

$$\dot{W}(t) = k\beta e^{-d\tau}\frac{x(t)y_2(t)}{1+\alpha x(t)+cy_2(t)} - d_1 y_2(t) - d_2 y_2^2(t). \tag{4.6}$$

Choosing $\varepsilon_1^* > 0$ small enough such that $\frac{k\beta(\eta_2^*-\varepsilon_1^*)e^{-d\tau}}{1+\alpha(M/k)+cM} > d_1$, we assume $\bar{y}_2 > y_2(t)$ for $t > T_1^*$. Accordingly, we obtain $x(t) > -(\mu + \beta\bar{y}_2)x(t)$ with regard to the first equation of model (2.6). Furthermore, We take into account the subsequent system:

$$\begin{cases} \dot{h}_4(t) = -(\mu + \beta\bar{y}_2)h_4(t), & t \neq (n+l-1)T,\ nT, \\ h_4(t^+) = (1+p)h_4(t), & t = (n+l-1)T, \\ h_4(t^+) = \left(1 - \dfrac{\lambda_{max}h_4(t)}{\delta + h_4(t)}\right)h_4(t), & t = nT, \end{cases} \tag{4.7}$$

and its globally asymptotically stable periodic solution is

$$\widetilde{h_4}(t) = \begin{cases} \left(\dfrac{\delta(1-\omega_2)}{(1-\lambda_{max})\omega_2^2 - \omega_2}\right)e^{-\mu_2(t-(n-1)T)}, & t \in ((n-1)T, (n+l-1)T], \\ (1+p)\left(\dfrac{\delta(1-\omega_2)}{(1-\lambda_{max})\omega_2^2 - \omega_2}\right)e^{-\mu_2(t-(n-1)T)}, & t \in ((n+l-1)T, nT], \end{cases} \tag{4.8}$$

where $\mu_2 = \mu + \beta\bar{y}_2$ and $\omega_2 = (1+p)e^{-\mu_2 T}$. Hence,

$$x(t) > \begin{cases} \left(\dfrac{\delta(1-\omega_2)}{(1-\lambda_{max})\omega_2^2 - \omega_2}\right)e^{-\mu_2 lT}, & t \in ((n-1)T, (n+l-1)T], \\ (1+p)\left(\dfrac{\delta(1-\omega_2)}{(1-\lambda_{max})\omega_2^2 - \omega_2}\right)e^{-\mu_2 T}, & t \in ((n+l-1)T, nT]. \end{cases} \tag{4.9}$$

That is to say $x(t) > \eta_2 = \left(\frac{\delta(1-\omega_2)}{(1-\lambda_{max})\omega_2^2-\omega_2}\right)e^{-\mu_2 lT} - \varepsilon_1^*$ for $t \in ((n-1)T, nT]$, $n > T_2^* > T_1^*$.

Let $y_m = \min_{t\in[t_0,t_0+\tau]} y_2(t) > 0$, and we discover that $y_2(t) \geq y_m$ holds for all $t > t_0 > T_2^*$. Then, we verify the fact by deriving a contradiction. There must be a T_0 such that $y_2(t) \geq y_m$ within the interval $t \in [t_0, t_0 + \tau + T_0]$, and $y_2(t_0 + \tau + T_0) = y_m$. By continuity, the derivative at this point meets $\dot{y}_2(t_0 + \tau + T_0) \leq 0$. Nevertheless, Theorem 3.6 and the second equation of model (2.6) show

$$\begin{aligned} \dot{y}_2(t_0+\tau+T_0) &= k\beta e^{-d\tau}\frac{x(t_0+T_0)y_2(t_0+T_0)}{1+\alpha x(t_0+T_0)+cy_2(t_0+T_0)} - d_1y_2(t_0+\tau+T_0) - d_2y_2^2(t_0+\tau+T_0) \\ &\geq \left(\frac{k\beta e^{-d\tau}\eta_2}{1+\alpha(M/k)+cM} - d_1 - d_2\bar{y}_2\right)y_m \\ &> 0. \end{aligned}$$

This is contradictory, so $y_2(t) \geq y_m$ for $t > t_0$. Similarly,

$$\dot{W}(t) \geq \left(\frac{k\beta e^{-d\tau}\eta_2}{1+\alpha(M/k)+cM} - d_1 - d_2\bar{y}_2\right)y_m > 0, \quad t > t_0.$$

Given that $W(t)$ is continuous on the interval $[0, +\infty)$ and the collection of points at which $W(t)$ is not differentiable is countable, it can be inferred that $W(t)$ tends to infinity as $t \to \infty$. This contradicts the uniform boundedness of $W(t)$. As a result, the original assumption is not valid. From this, we can further infer two scenarios: (i) $y_2(t) \geq \bar{y}_2$ for sufficiently large t; (ii) $y_2(t)$ fluctuates around $\bar{y}_2$ when t is

sufficiently large.

We define $m_1 = \min\left\{\frac{\bar{y}_2}{2}, \bar{y}_2 e^{-(d_1+d_2M)(T+\tau)}\right\}$, with the aim to demonstrate that $y_2(t) \geq m_1$ for sufficiently huge t. In case (i), the conclusion can be easily obtained. For case (ii), assume t_1 and t_2 are sufficiently large moments satisfying $y_2(t_1) = y_2(t_2) = \bar{y}_2$ and $y_2(t) < \bar{y}_2$ when $t \in (t_1, t_2)$. If $t_2 - t_1 \leq T + \tau$, since $\dot{y_2}(t) \geq -(d_1 + d_2M)y_2(t)$, it follows that $y_2(t) \geq m_1$ in the interval $[t_1, t_2]$. Thus, if $t_2 - t_1 > T + \tau$, we own $y_2(t) \geq m_1$ for $t \in [t_1, t_1 + T + \tau]$. Hence, by strictly adhering to the reasoning line in the proof of the preceding claim, we can deduce that $y_2(t) \geq m_1$ in the interval $[t_1, t_2]$. Therefore, $y_2(t) \geq m_1$ holds for all t in all possible situations. It should be noted that the definition of m_1 is independent on the solution of model (2.6).

By virtue of Theorem 3.6 and the initial equation in the model (2.6), it is straightforward to obtain that $x(t) \geq -(\mu + \beta M)x(t)$. Evidently, when n is sufficiently large, we get

$$x(t) \geq \left(\frac{\delta(1-\omega_3)}{(1-\lambda_{max})\omega_3^2 - \omega_3}\right) e^{-\mu_3 lT} - \varepsilon^* = m_2, \ t \in ((n-1)T, nT], \tag{4.10}$$

where $\mu_3 = \mu + \beta M$, $\omega_3 = (1+p)e^{-\mu_3 T}$ and ε^* is small enough.

To summarize, we arrive at the conclusion:

$$D = \{(x(t), y_2(t)) \mid m_2 \leq x(t) \leq M/k, \ m_1 \leq y_2(t) \leq M\},$$

represents a compact and bounded region. This region maintains a positive distance from the coordinate hyperplanes. All solutions of model (2.6) will eventually enter D and remain within it indefinitely. Thus, the demonstration is concluded.

From the above derivations, we obtain a critical threshold for the permanence of system (2.6). Rearranging the threshold expressions yields the feasible parametric constraints for coexistence of the two species, as summarized in Table 2.

Table 2. The critical threshold of key parameters ensuring the persistence of model (2.6).

The conditions for persistence	
$L_2 < 1$	$L_2 = \frac{d_1}{k\beta\eta_2^* e^{-d\tau}}\left(1 + \left(\frac{\alpha}{k} + c\right)M\right)$
$\lambda_{\max} < \lambda_{\max}^*$	$\lambda_{\max}^* = 1 - \frac{k\beta\delta(1-w)\exp(-\mu lT - d\tau) - \delta(1-w)\left(\frac{\alpha}{k} + c\right)\frac{kpd_1}{\exp(qT)-1}}{w^2\left(d_1 + \left(\frac{\alpha}{k} + c\right)d_1\frac{Q}{q}\right)} + \frac{1}{w}$
$\tau < \tau^*$	$\tau^* = -\frac{1}{d}\ln\frac{d_1\left(1 + \left(\frac{\alpha}{k} + c\right)M\right)}{k\beta\eta_2^*}$
$c < c^*$	$c^* = \frac{k\beta\eta_2^*\exp(-d\tau) - d_1}{d_1 M} - \frac{\alpha}{k}$

5. Numerical simulation and discussions

To further explore the theoretical findings, numerical simulations will be performed subsequently. We choose a set of fixed parameter values as follows:

$$\mu = 0.3, \quad \alpha = c = 0.1, \quad \beta = 1.2, \quad k = 0.8, \quad d = d_2 = 0.3,$$
$$d_1 = 0.2, \quad \delta = 0.5, \quad p = 1.6, \quad l = 0.3, \quad x(0) = y_1(0) = y_2(0) = 0.2.$$

Choosing $T = 2.5$, $\tau = 0.8$, and $\lambda_{max} = 0.35$, all the requirements of Theorem 4.2 are met and $L_2 = 0.8102 < 1$. That is to say, model (2.6) is permanent (Figure 1).

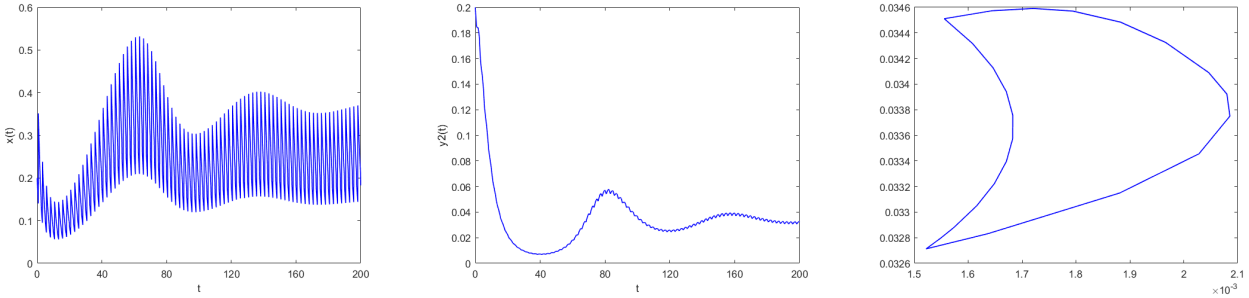

(a) Time-series depicting the prey population $x(t)$

(b) Time-series depicting the mature predator population $y_2(t)$

(c) Phase portrait of the permanence

Figure 1. The permanence of model (2.6) at $\mu = 0.3, \alpha = c = 0.1, \beta = 1.2, k = 0.8, d = d_2 = 0.3, d_1 = 0.2, \delta = 0.5, p = 1.6, l = 0.3, \tau = 0.8, T = 2.5, \lambda_{max} = 0.35$, and $L_2 = 0.8102 < 1$.

To analyze how the harvesting intensity influences model (2.6), we adjust the maximum harvesting effort λ_{max} from 0.35 to 0.8 while keeping all other parameters unchanged. The requirements of Theorem 4.1 are fulfilled ($L_1 = 1.0360 > 1$), meaning the prey population persists in the long term and the predator tends to extinction. In addition, the outcome stays consistent under different initial value conditions in Figure 2(c). This is not inconsistent with the realistic ecological laws. Excessive harvesting of high-value fish often starves their natural enemies leading to a sharper population decline. Take Carcharodon carcharias for instance: its survival and reproduction rely heavily on sufficient prey, among which the Trachurus capensis serves as a primary food source. Overfishing of Trachurus capensis has driven the rapid decline of Carcharodon carcharias. In turn, following the sharks' depletion, the Trachurus capensis also dropped markedly. Therefore, overfishing not only damages biodiversity but also hinders the sustainable development of fisheries.

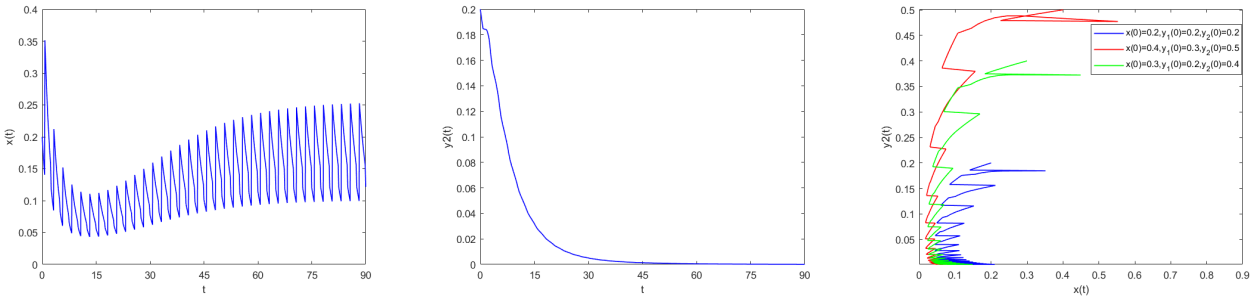

(a) Time-series depicting the prey population $x(t)$

(b) Time-series depicting the mature predator population $y_2(t)$

(c) Phase portrait of the predator-extinction periodic solution

Figure 2. The globally attractive periodic solution $(\widetilde{x_2}(t), 0)$ of model (2.6) at $\mu = 0.3, \alpha = c = 0.1, \beta = 1.2, k = 0.8, d = d_2 = 0.3, d_1 = 0.2, \delta = 0.5, p = 1.6, l = 0.3, \tau = 0.8, T = 2.5, \lambda_{max} = 0.8$, and $L_1 = 1.0360 > 1$.

Let $T = 3$, $\tau = 0.8$ and $\lambda_{max} = 0.35$. According to Theorem 4.1, we can infer that the predator-vanishing periodic solution of model (2.6) possesses global attraction, as shown in Figure 3. Evidently, an extended pulse period breaks the coexistence state of the two populations.

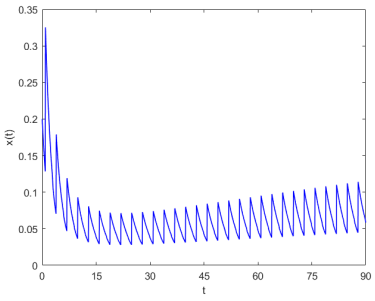

(a) Time-series depicting the prey population $x(t)$

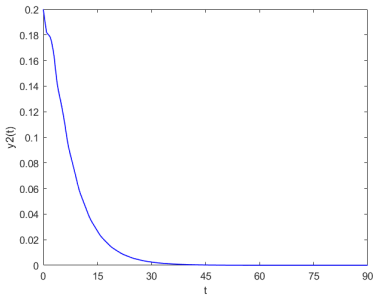

(b) Time-series depicting the mature predator population $y_2(t)$

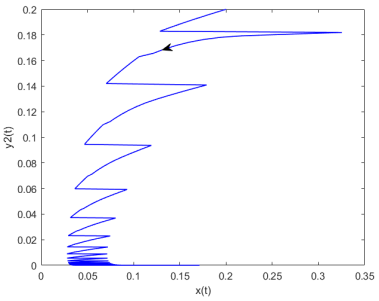

(c) Phase portrait of the predator-extinction periodic solution

Figure 3. The globally attractive periodic solution $(\widetilde{x_2}(t), 0)$ of model (2.6) at $\mu = 0.3, \alpha = c = 0.1, \beta = 1.2, k = 0.8, d = d_2 = 0.3, d_1 = 0.2, \delta = 0.5, p = 1.6, l = 0.3, \tau = 0.8, T = 3, \lambda_{max} = 0.35$, and $L_1 = 1.5464 > 1$.

Exploring the influence of maturation delay on the system's dynamic behavior constitutes another critical analysis dimension. We change τ from 0.8 to 5.2 without altering other parameters and find that the predator population in model (2.6) tends to extinction (Figure 4). This is because juvenile fish that require a long maturation period are more vulnerable to complex environmental fluctuations, which reduces their survival rate. As a result, the maximum adult recruitment rate ($k\beta e^{-d\tau}$) may fall below the adult mortality rates (d_1, d_2), leading to population extinction.

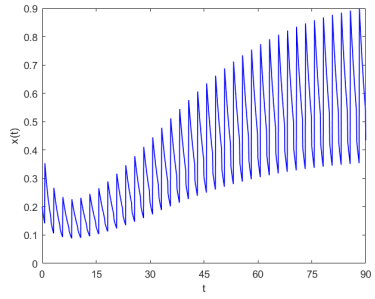

(a) Time-series depicting the prey population $x(t)$

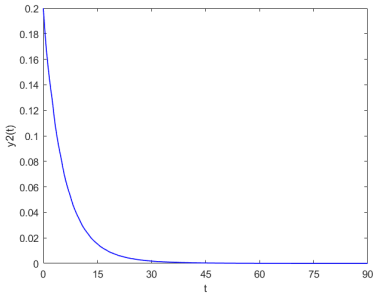

(b) Time-series depicting the mature predator population $y_2(t)$

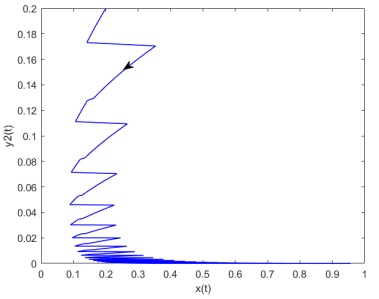

(c) Phase portrait of the predator-extinction periodic solution

Figure 4. The globally attractive periodic solution $(\widetilde{x_2}(t), 0)$ of model (2.6) at $\mu = 0.3, \alpha = c = 0.1, \beta = 1.2, k = 0.8, d = d_2 = 0.3, d_1 = 0.2, \delta = 0.5, p = 1.6, l = 0.3, \tau = 5.2, T = 2.5, \lambda_{max} = 0.35$, and $L_1 = 1.0370 > 1$.

Afterwards, we further investigate the bifurcation parameter diagram to analyze how the pulse effect impacts the dynamic behavior of model (2.6). We analyse the impact of maximum pulsed harvesting intensity λ_{max} as the bifurcation parameter on the dynamics of model (2.6) (Figure 5). It can be seen that λ_{max} is a valuable parameter that governs the transition of model (2.6) from the chaotic state to T-periodic solution. When λ_{max} is small, the system exhibits rich and complex dynamical features; as this parameter gradually increases, the system converges to a positive periodic solution, which implies that prey and predator populations achieve coexistence.

Next, we select the birth rate p of prey population as the bifurcation parameter to explore its

influence on dynamic properties. Fix a set of parameters: $\mu = 0.3$, $\beta = 4$, $\alpha = 0.65$, $c = 0.3$, $k = 0.12$, $d = 0.3$, $\tau = 0.3$, $d_1 = 0.2$, $d_2 = 0.3$, $\delta = 4$, $\lambda = 0.8$, $l = 0.3$, $T = 1$ and $x(0) = y_1(0) = y_2(0) = 1.5$, and the corresponding bifurcation picture can be seen in Figure 6. We can observe from Figure 6 that the fishery management model shows complex dynamic features as a bifurcation parameter p varies. When p is relatively small, the prey and predator populations go extinct simultaneously; as p increases slightly, the system converges to positive periodic solution, enabling the two populations to coexist. With further increases in p, the system transitions to a chaotic regime; as p continues to increase, the system settles into a new positive periodic solution, restoring coexistence between the two populations.

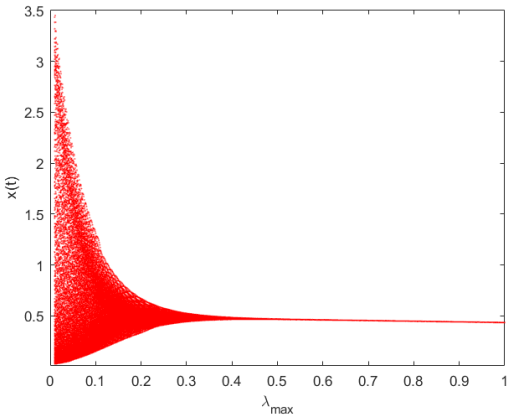

(a) Bifurcation picture of $x(t)$ for the bifurcation parameter λ_{max}

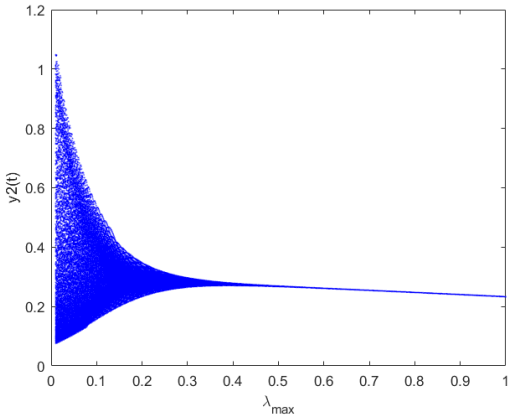

(b) Bifurcation picture of $y_2(t)$ for the bifurcation parameter λ_{max}

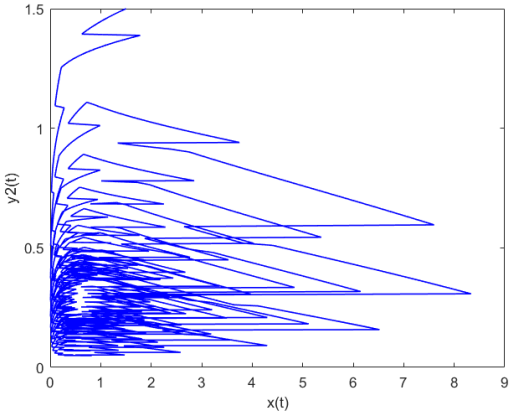

(c) The phase portrait at $\lambda_{max} = 0.16$

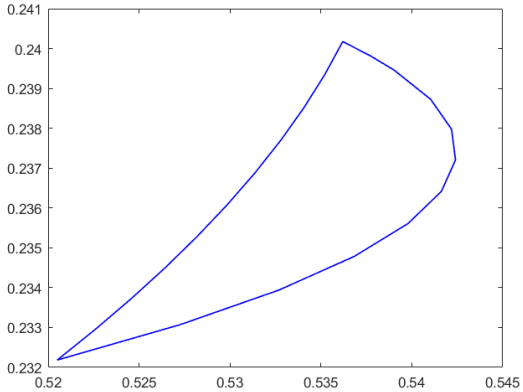

(d) The phase portrait at $\lambda_{max} = 0.9$;

Figure 5. The bifurcation diagram of model (2.6) at $\mu = 0.35$, $\beta = 3$, $\alpha = 0.15$, $c = 0.3$, $k = 0.6$, $d = 0.3$, $\tau = 5$, $d_1 = 0.2$, $d_2 = 0.3$, $\delta = 3$, $p = 2$, $l = 0.3$, $T = 1$, $x(0) = y_1(0) = y_2(0) = 1.5$, and $0 < \lambda_{max} < 1$.

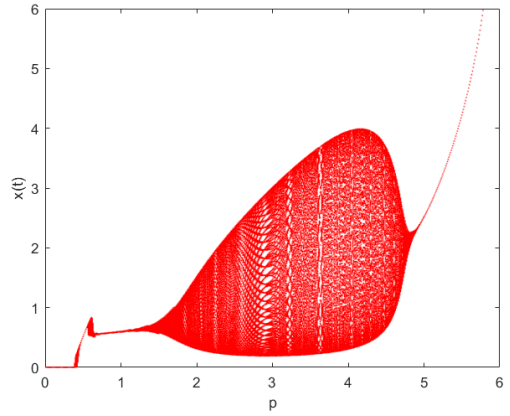

(a) Bifurcation picture of $x(t)$ for the bifurcation parameter p

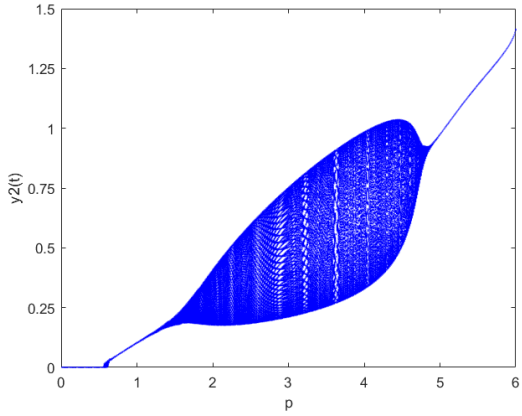

(b) Bifurcation picture of $y_2(t)$ for the bifurcation parameter p

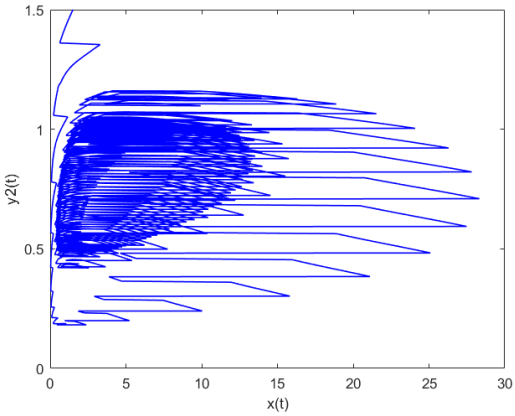

(c) The phase portrait at $p = 4.5$

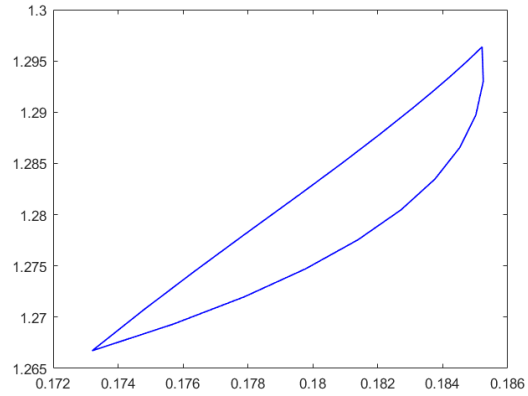

(d) The phase portrait at $p = 5.8$

Figure 6. The bifurcation diagram of model (2.6) at the $\mu = 0.3, \beta = 4, \alpha = 0.65$, $c = 0.3$, $k = 0.12$, $d = 0.3$, $\tau = 0.3$, $d_1 = 0.2$, $d_2 = 0.3$, $\delta = 4$, $\lambda = 0.8$, $l = 0.3$, $T = 1$, $x(0) = y_1(0) = y_2(0) = 1.5$, and $0 \leq p \leq 6$.

6. Conclusions

As an important industry related to food security, ecological stability, and the livelihoods of numerous practitioners, fisheries have received widespread attention regarding their sustainable development. Implementing scientific and effective fishery management strategies not only meet the current demands but also ensure the continuous enrichment of fishery resources in the future. To achieve this objective, our primary focus is to explore a fishery management model incorporating delayed stage-structure for predator populations, along with impulsive nonlinear harvesting and pulse birth for prey populations. Initially, we verify the non-negativity and uniform boundedness of the system's solutions. In Section 4, we further demonstrate the existence and global attraction of the predator-vanish periodic solution, as well as the system's persistence. Through numerical simulations, we confirm the accuracy of the theoretical findings. In addition, we discover that higher harvesting

intensity λ_{max}, longer pulse period T, or increased maturation delay τ can disrupt the system's stability and drive predator population to extinction. Moreover, we notice that impulsive birth rate p and maximum harvesting intensity λ_{max} can influence the system's dynamic characteristics, giving rise to phenomena like chaos. Thus, the improper interventions can bring about a shift from the coexistence of two populations to the disappearance of the predator population, which leads to an ecosystem imbalance. In fishery management, capping harvesting intensity below the critical tolerance threshold is fundamental to population stability. Scientific alternation of fishing and moratorium periods enables fish stocks adequate time to recover. Targeted conservation of commercially valuable juvenile fish reduces unnecessary early-life mortality and sustains adult recruitment. By maintaining population abundance within a balanced range to ensure long-term viability, we can achieve sustainable development of fisheries.

In future research, we will adopt rigorous mathematical methods to further explore potential biological mechanisms, such as fear effects, refuge effects, and spatial diffusion, to construct population dynamic models that better reflect realistic ecological contexts. Furthermore, exploring the scientific regulation of fishing intensity, fishing cycles, and moratorium strategies via mathematical models also holds important research value and practical significance.

Author contributions

Shirui Zhang: Methodology, Writing-original draft, Software; Jianjun Jiao: Funding acquisition, Supervision; Guiyu Wu: Conceptualization, Writing-review & editing; Bingying Gao: Validation. All authors have read and approved the final version of the manuscript for publication.

Use of Generative-AI tools declaration

The authors declare that no Artificial Intelligence (AI) tools were used in the composition of this article.

Acknowledgments

This work was supported by National Natural Science Foundation of China (No.12261018) and Guizhou University of Finance and Economics Graduate Program (2025BAZYSY215).

Conflict of interest

The authors declare no competing interests.

References

1. W. Xu, W. Long, Multi-strategy enhanced grey wolf optimizer for numerical optimization and its application to feature selection, *J. Math. Interdiscip. Appl.*, **1** (2025), 51–71. https://doi.org/10.62762/JMIA.2025.522565

2. B. Li, Q. Zhang, Analysis of trajectory structure and GAS for a high-order nonlinear difference equation, *J. Math. Interdiscip. Appl.*, **2** (2026), 28–35. https://doi.org/10.62762/JMIA.2025.554313
3. Y. Tian, Y. Gao, K. Sun, A fishery predator-prey model with anti-predator behavior and complex dynamics induced by weighted fishing strategies, *Math. Biosci. Eng.*, **20** (2023), 1558–1579. https://doi.org/10.3934/mbe.2023071
4. L. Wu, J. Jiao, X. Dai, Z. Zhou, Dynamical analysis of an ecological aquaculture management model with stage-structure and nonlinear impulsive releases for larval predators, *AIMS Math.*, **9** (2024), 29053–29075. https://doi.org/10.3934/math.20241410
5. G. Hua, T. Yuan, S. Kaibiao, S. Xinyu, Study on dynamic behavior of two fishery harvesting models: effects of variable prey refuge and imprecise biological parameters, *J. Appl. Math. Comput.*, **69** (2025), 4243–4268. https://doi.org/10.1007/s12190-023-01925-0
6. B. Zhang, X. Liu, Y. Wei, Predator-prey systems with a variable habitat for predators in advective environments, *Stud. Appl. Math.*, **153** (2024), e12758. https://doi.org/10.1111/sapm.12758
7. X. Bo, G. Lv, W. Liu, A. Moussaoui, Optimal harvest control of predator–prey systems in fisheries with stage structure and additional food supply, *J. Biol. Syst.*, **33** (2025), 221–246. https://doi.org/10.1142/S0218339025500032
8. Z. Zhou, J. Jiao, X. Dai, Dynamics of an aquaculture model with impulsive harvesting of predators and density-dependent nonlinear release of prey, *Complexity*, **2025** (2025), 2274956. https://doi.org/10.1155/cplx/2274956
9. S. Biswas, B. Ahmad, S. Khajanchi, Exploring dynamical complexity of a cannibalistic eco-epidemiological model with multiple time delay, *Math. Methods Appl. Sci.*, **46** (2023), 4184–4211. https://doi.org/10.1002/mma.8749
10. L. Wu, J. Jiao, X. Dai, Z. Zhou, Dynamical analysis of an ecological aquaculture management model with stage-structure and nonlinear impulsive releases for larval predators, *AIMS Math.*, **9** (2024), 29053–29075. https://doi.org/10.3934/math.20241410
11. W. Sun, N. Wang, N. Li, Y. Lv, S. Liu, A structured predator–prey model with a state-dependent maturation period, *Int. J. Bifurc. Chaos*, **35** (2025), 2550123. https://doi.org/10.1142/S0218127425501238
12. H. Jiao, S. Meleshko, Analysis of a pest-natural enemy model with time delay in impulsive releasing natural enemy, *J. Math. Interdiscip. Appl.*, **1** (2025), 20–28. https://doi.org/10.62762/JMIA.2025.442174
13. J. Jiao, Y. Xiao, Dynamics of a pest-natural enemy model with natural enemy periodic migration described by time delay, *Nonlinear Anal. Real World Appl.*, **87** (2026), 104454. https://doi.org/10.1016/j.nonrwa.2025.104454
14. R. Arditi, L. R. Ginzburg, Coupling in predator-prey dynamics: ratio-dependence, *J. Theor. Biol.*, **139** (1989), 311–326. https://doi.org/10.1016/S0022-5193(89)80211-5
15. G. Huisman, R. J. De Boer, A formal derivation of the Beddington functional response, *J. Theor. Biol.*, **185** (1997), 389–400. https://doi.org/10.1006/jtbi.1996.0318

16. J. R. Beddington, Mutual interference between parasites or predators and its effect on searching efficiency, *J. Anim. Ecol.*, **44** (1975), 331–340. https://doi.org/10.2307/3866

17. D. L. DeAngelis, R. A. Goldstein, R. V. O'Neill, A model for tropic interaction, *Ecology*, **56** (1975), 881–892. https://doi.org/10.2307/1936298

18. C. S. Holling, The functional response of predators to prey density and its role in mimicry and population regulation, *Mem. Entomol. Soc. Can.*, **97** (1965), 5–60. https://doi.org/10.4039/entm9745fv

19. C. Li, X. Feng, Y. Wang, X. Wang, Complex dynamics of Beddington–DeAngelis-type predator-prey model with nonlinear impulsive control, *Complexity*, **2020** (2020), 8829235. https://doi.org/10.1155/2020/8829235

20. X. Feng, C. Sun, W. Yang, C. Li, Dynamics of a predator-prey model with nonlinear growth rate and B-D functional response, *Nonlinear Anal. Real World Appl.*, **70** (2023), 103766. https://doi.org/10.1016/j.nonrwa.2022.103766

21. X. Feng, M. Liu, Y. Jiang, D. Li, Dynamics and stability of a fractional-order tumor–immune interaction model with B-D functional response and immunotherapy, *Fractal Fract.*, **7** (2023), 200. https://doi.org/10.3390/fractalfract7020200

22. Q. Quan, M. Wang, J. Jiao, X. Dai, Dynamics of a predator–prey fishery model with birth pulse, impulsive releasing and harvesting on prey, *J. Appl. Math. Comput.*, **70** (2024), 3011–3031. https://doi.org/10.1007/s12190-024-02081-9

23. L. Ling, W. Wang, Dynamics of a Ivlev-type predator–prey system with constant rate harvesting, *Chaos Soliton. Fract.*, **41** (2009), 2139–2153. https://doi.org/10.1016/j.chaos.2008.08.024

24. J. Jiao, L. Chen, S. Cai, Dynamical analysis of a biological resource management model with impulsive releasing and harvesting, *Adv. Differ. Equ.*, **2012** (2012), 9. https://doi.org/10.1186/1687-1847-2012-9

25. G. Wu, J. Jiao, X. Dai, Pest control model with delayed stage structure for pest and nonlinearly impulsive releasing predator, *J. Math.*, **2025** (2025), 5547439. https://doi.org/10.1155/jom/5547439

26. C. Li, S. Tang, Analyzing a generalized pest-natural enemy model with nonlinear impulsive control, *Open Math.*, **16** (2018), 1390–1411. https://doi.org/10.1515/math-2018-0114

27. D. D. Bainov, P. S. Simeonov, *Impulsive differential equations: asymptotic properties of the solutions*, Singapore: World Scientific, 1995.

AIMS Press